Molecular Biology of the Cell
Vol. 20, 1705–1714, March 15, 2009

The SM Protein Car/Vps33A Regulates SNARE-mediated Trafficking to Lysosomes and Lysosome-related Organelles

Mohammed A. Akbar,* Sanchali Ray,† and Helmut Krämer*†

Departments of *Neuroscience and †Cell Biology, University of Texas Southwestern Medical Center, Dallas, TX 75390-9111

Submitted March 25, 2008; Revised November 25, 2008; Accepted January 9, 2009
Monitoring Editor: Marcos Gonzalez-Gaitan

The SM proteins Vps33A and Vps33B are believed to act in membrane fusions in endosomal pathways, but their specific roles are controversial. In *Drosophila*, Vps33A is the product of the *carnation* (*car*) gene. We generated a null allele of *car* to test its requirement for trafficking to different organelles. Complete loss of *car* function is lethal during larval development. Eye-specific loss of Car causes late, light-independent degeneration of photoreceptor cells. Earlier in these cells, two distinct phenotypes were detected. In young adults, autophagosomes amassed indicating that their fusion with lysosomes requires Car. In eye discs, endocytosed receptors and ligands accumulate in Rab7-positive prelysosomal compartments. The requirement of Car for late endosome-to-lysosome fusion in imaginal discs is specific as early endosomes are unaffected. Furthermore, lysosomal delivery is not restored by expression of dVps33B. This specificity reflects the distinct pattern of binding to different Syntaxins in vitro: dVps33B predominantly binds the early endosomal Avl and Car to dSyntaxin16. Consistent with a role in Car-mediated fusion, dSyntaxin16 is not restricted to Golgi membranes but also present on lysosomes.

INTRODUCTION

Membrane fusion events are necessary for cargo to move between distinct endocytic compartments. The specificity of these fusion events is controlled by multiple elements. First, tethering factors force membranes into sustained proximity before fusion is initiated (Whyte and Munro, 2002; Cai *et al*., 2007). A second contribution to the specificity of fusion comes from the restricted combinations in which *N*-ethylmaleimide-sensitive factor attachment protein receptors (SNAREs) combine preceding fusion (McNew *et al*., 2000; Jahn and Scheller, 2006; Bethani *et al*., 2007). A third element of specificity is provided by the family of Sec1/Munc18-related SM proteins, which were first identified based on genetic screens in *Drosophila*, *Caenorhabditis elegans*, and yeast (Beadle and Ephrussi, 1936; Brenner, 1974; Novick and Schekman, 1979). The interactions of SM proteins with SNAREs are complex (Carpp *et al*., 2006) but seem to be required for all SNARE-mediated fusion events (Jahn *et al*., 2003; Toonen and Verhage, 2003).

SM proteins add specificity and efficiency to membrane docking and fusion events by directly interacting with individual SNARE proteins and also with assembled SNARE complexes (Rizo and Sudhof, 2002; Hong, 2005; Dulubova *et al*., 2007; Shen *et al*., 2007). For example, yeast Vps33 is required for early endosomal fusion events (Peterson and Emr, 2001; Subramanian *et al*., 2004) and also for fusions of vacuolar membranes with late endosomes, other vacuoles, or autophagosomes (Banta *et al*., 1990; Seals *et al*., 2000; Klionsky, 2005). During such fusion reactions, Vps33 participates in two distinct steps: early in the tethering of vesicles to the target membrane and later in the SNARE-mediated fusion (Wang *et al*., 2003).

Like other SM proteins (Dulubova *et al*., 2002, 2007; Carpp *et al*., 2006; Latham *et al*., 2006), Vps33 interacts with SNAREs: Pep12 during early endosomal fusion (Subrahmanyam *et al*., 2003) and Vam3 (Sato *et al*., 2000) or Vam7 (Stroupe *et al*., 2006) during vacuolar fusions. These interactions may be indirect, however, because Vps33 is part of two protein complexes: the CORVET complex (short for class C core vacuole/endosome tethering) during endosomal fusions (Peplowska *et al*., 2007) and the HOPS complex (for Homotypic Vacuolar Protein Sorting) during vacuolar fusions (Seals *et al*., 2000; Wurmser *et al*., 2000). Both of these complexes share a core comprising the group C vacuolar protein sorting (Vps) proteins Vps11, Vps16, Vps18, and Vps33 (Rieder and Emr, 1997). This core is modified by the accessory subunits Vps3 and Vps8 in the CORVET complex (Subramanian *et al*., 2004; Peplowska *et al*., 2007) or Vps39/Vam6 and Vps41/Vam2 in the HOPS complex (Seals *et al*., 2000; Wurmser *et al*., 2000). Interactions among the core Vps-C proteins are well conserved in vertebrates (Kim *et al*., 2001; Richardson *et al*., 2004) and invertebrates (Sevrioukov *et al*., 1999; Pulipparacharuvil *et al*., 2005).

Metazoan genomes encode two Vps33 homologues (Pevsner *et al*., 1996) and loss of function models have been described for both in different species. Knockdown of Vps33B in zebrafish results in underdeveloped bile ducts (Matthews *et al*., 2005). Similarly, mutations in the human *vps33B* gene cause defects in motor units, kidney epithelia, and bile secretion (Gissen *et al*., 2004), a triad of symptoms characteristic of arthrogryposis-renal dysfunction-cholestasis syndrome (ARC). Strikingly, kidney and liver cells from

This article was published online ahead of print in *MBC in Press* (http://www.molbiolcell.org/cgi/doi/10.1091/mbc.E08–03–0282) on January 21, 2009.

Address correspondence to: Helmut Krämer (hkrame@mednet.swmed.edu).

ARC patients mislocalize some proteins normally restricted to the apical surface (Gissen *et al.*, 2004).

These phenotypes are distinct from those observed for mutations in Vps33A in mice and flies. A point mutation in the murine *buff* gene causes several defects typical for Hermansky–Pudlak syndrome, such as reduced pigmentation and prolonged bleeding time due to defects in secretory granules of platelets (Suzuki *et al.*, 2003). Similarly, in *Drosophila* a single amino acid change in the Vps33A homologue is responsible for the *carnation*[1] (*car*[1]) eye color mutation (Sevrioukov *et al.*, 1999). Eye pigmentation defects also accompany the functional loss of other homologues of HOPS subunits, particularly *deep orange* (*dor*), the homologue of *vps18* (Shestopal et al., 1997); *light*, the homologue of *vps41* (Warner *et al.*, 1998); and dVps16A (Pulipparacharuvil *et al.*, 2005). Beyond pigmentation, *Drosophila* HOPS complex subunits are also required for lysosomal delivery of different cargoes and the fusion of lysosomes with autophagosomes (Sevrioukov *et al.*, 1999; Sriram *et al.*, 2003; Pulipparacharuvil *et al.*, 2005; Lindmo *et al.*, 2006).

To which extend the two Vps33 homologues contribute to different fusion events in the endosomal/lysosomal system (Figure 1A) is not well defined yet. Some studies pointed to a role of Car/Vps33A as part of the HOPS complex in lysosomal delivery and autophagosome fusion (Sriram *et al.*, 2003; Pulipparacharuvil *et al.*, 2005; Simonsen *et al.*, 2007). By contrast, other studies suggested that the role of Vps33A homologues are restricted to the delivery of cargo to melanosomes and lysosome-related organelles (LROs), whereas Vps33B homologues function during endosomal and lysosomal fusions (Suzuki *et al.*, 2003; Gissen *et al.*, 2005). To clarify the role of Vps33 homologues, we have generated a null allele of *car*. Its analysis revealed that Car is required not only for pigmentation but also for the delivery of different cargoes to lysosomes and for the normal subcellular distribution of Rab7-positive late endosomes.

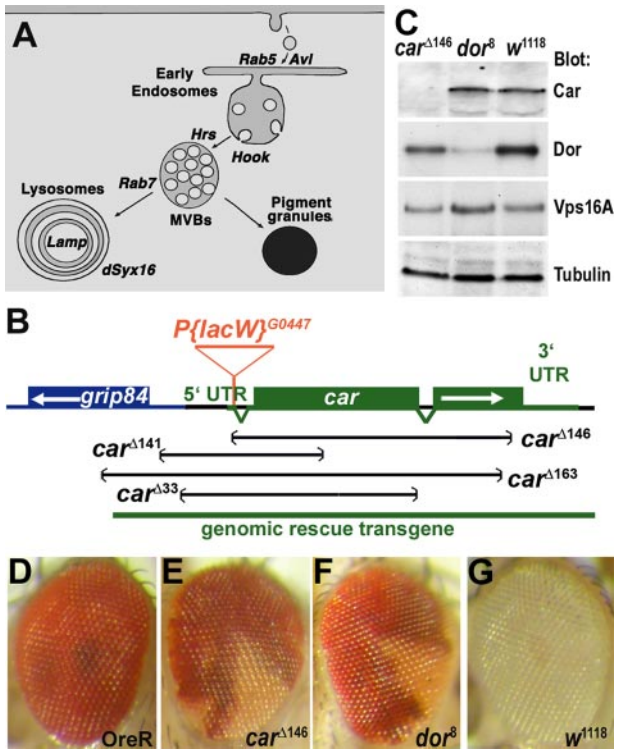

Figure 1. Car is an essential gene. (A) Cartoon shows endocytic intermediates and the markers used in this study for their detection. (B) Diagram of the *car* genomic region. Imprecise excision of the P-element P[lacW]^{G0447} in the 5′ UTR of the *car* yielded the indicated deletions. Molecular analysis revealed that *car*$^{\Delta 146}$ removed almost the entire *car* coding unit without extending into the *grip84* gene. The *car*$^{\Delta 146}$ deletion was used for further studies. Lethality of the *car*$^{\Delta 146}$ chromosome was rescued by the indicated genomic rescue construct. (C) Western blot of lysates (20 μg of protein) from *car*$^{\Delta 146}$, *dor*^{8} and *w*^{1118} second instars were probed with antibodies against Car, Dor, dVps16A, or α-tubulin as control. (D–G) Micrographs of adult eyes reveal reduced pigmentation of clones of *car*$^{\Delta 146}$ (E) or *dor*^{8} (F) homozygous mutant cells compared with Oregon R (D) or *w*^{1118} (G) control eyes. Genotypes: *car*$^{\Delta 146}$, *dor*^{8}, and *w*^{1118} (C), Oregon R (D), *w*$^{+}$ *car*$^{\Delta 146}$ FRT^{19A}/*w*$^{+}$ FRT^{19A}; hsFLP (E), *w*$^{+}$ *dor*^{8} FRT^{19A}/*w*$^{+}$ FRT^{19A}; hsFLP (F), *w*^{1118} (G).

MATERIALS AND METHODS

Molecular Biology

For expression in S2 cells, plasmids encoding epitope-tagged versions of full-length Car and dVps33B under control of the metallothionein promoter have been described previously (Pulipparacharuvil *et al.*, 2005). Similar expression constructs were prepared for the Syntaxins Avl, dSyntaxin8, dSyntaxin13, and dSyntaxin16 by using polymerase chain reaction (PCR), but each of their respective transmembrane domains were replaced with the BN tag (amino acids 59–77 of the Boss protein: TSPTKKSAPLRITKPQPTS). Antibodies specifically recognizing this epitope have been described previously (Krämer *et al.*, 1991). S2 cells were transfected and 24 h later addition of 0.7 mM Cu_2SO_4-induced expression (Bunch *et al.*, 1988). Sixteen to 24 h after induction, S2 cells were lysed in a buffer containing 10 mM HEPES/KOH, pH 7.4, 143 mM KCl, 5 mM $MgCl_2$, Complete EDTA-free protease inhibitor mix (Roche Applied Science, Indianapolis, IN), 1 mM dithiothreitol, and 1% Triton X-100. Lysates were spun at 20,000 $\times$ *g* for 20 min, and the cleared supernatant was used for immunoprecipitation assays as described previously (Pulipparacharuvil *et al.*, 2005).

Fly Work

Transgenic flies were generated with pUASt vectors (Brand and Perrimon, 1993) containing cDNAs encoding Car (Sevrioukov *et al.*, 1999), a Myc-tagged dVps33B or green fluorescent protein (GFP)-lysosomal-associated membrane protein (Lamp) 1 (Pulipparacharuvil *et al.*, 2005). Expression of these constructs was driven by P[GMR-Gal4] (Hay *et al.*, 1994), P[ey-Gal4] (Hazelett *et al.*, 1998), or P[da-gal4] (Wodarz *et al.*, 1995), or it was under control of the MARCM system (Lee and Luo, 2001) as indicated. The respective fly lines were obtained from the Bloomington Stock Center (Department of Biology, Indiana University, Bloomington, IN). Lines expressing Rab5-cyan fluorescent protein (CFP), Rab7-yellow fluorescent protein (YFP), or Rab11-YFP at low levels under control of the tubulin promoter (Marois *et al.*, 2006) were a generous gift by S. Eaton (MPI, Dresden, Germany). A ubiquitously expressed marker for lysosomes was generated by expressing GFP-LAMP1 (Pulipparacharuvil *et al.*, 2005) under control of the tubulin promoter. A 4.4-kb genomic fragment containing the *car* genomic region was generated using the primers ccgctcgAGCGCTGAAAGGCTAGTGGAAC and cggaattcACTTTTGTTTGGAATGCTTTCCGTTT and inserted into the XbaI and EcoRI sites of the pCasper4 vector for establishment of transgenic lines.

For generation of the *car* null allele, we started with the *car*^{G0447} allele in which a P element (EPgy2) is inserted ~150 base pairs upstream of the *Car* start codon (Peter *et al.*, 2002). This P element was mobilized using standard procedures. The resulting precise excisions were wild type. Imprecise excisions were initially detected by noncomplementation of *car*[1], and subsequently the extent of the deletion was determined using PCR followed by sequencing. For Western blots of *car*$^{\Delta 146}$ and *dor*^{8} lysates, hemizygous larvae were recognized by the absence of the GFP-tagged FM7 balancer (Casso *et al.*, 2000).

To test for genetic interactions between *car* and *dSyx16*, we used the deficiency Df(1)Exel6254, which eliminates dSyx16 but did not exhibit genetic interactions with +/*car*[1] flies. Similarly, a dSyx16-RNA interference (RNAi) transgene from the Vienna stock center failed to interact with *car*[1].

Histology and Microscopy

Imaginal discs were stained with antibodies against Dor (DorY81, 1:100), Avl (dSyx7-44, 1:1000), and dVps16A (vps16-67, 1:1000) or the Myc epitope (9E10, 1:500) as described previously (Pulipparacharuvil *et al.*, 2005). Other antibodies used were against Car (Car-1454, 1:1000; Sevrioukov *et al.*, 1999), Boss (rabbit NN1, 1:2000; αboss1, 1:500; Krämer *et al.*, 1991), Hook (1:500; Krämer and Phistry, 1996), Delta (GP581, 1:1000; mAb202, 1:50; Parks *et al.*, 1995), Hrs (N-term, 1:300; Lloyd *et al.*, 2002), gp150 (1:75; Li *et al.*, 2003), Notch (mAbC17.9C6, 1:50; Fehon *et al.*, 1990); Elav (9F8A9, 1:100; O'Neill *et al.*, 1994),

dSyntaxin16 (1:100; Xu *et al*., 2002), γ-tubulin (GTU-88, 1:100; Sigma-Aldrich, St. Louis, MO), GFP (1:1000; Invitrogen, Carlsbad, CA), Golgi protein (7H6D7C2 1:200; EMD Biosciences, San Diego, CA), intermediate chain of cytoplasmic dynein (IC74 1:100; Covance Research Products, Princeton, NJ). Localization of key markers is indicated in Figure 1A.

Live internalization assays were performed as described by Le Borgne and Schweisguth (2003). In brief, freshly retrieved eye discs were incubated in Schneider's medium containing antibodies against the extracellular domain of Delta (mAb202) for 20 min at 4°C. Subsequently, after three brief washes and the indicated chase time, discs were fixed, permeabilized, and the location of internalized antibodies was compared with that of total Delta (GP581).

Secondary antibodies conjugated to the indicated Alexa dyes were detected using 63 × numerical aperture (NA) 1.4 or 40× NA 1.3 lenses on an LSM510 Meta confocal microscope (Carl Zeiss, Thornwood, NY). Its Meta detector allowed for the spectral separation of CFP, enhanced (e)GFP, and YFP. All digital images were imported into Photoshop (Adobe Systems, Mountain View, CA) and adjusted for gain and contrast. For light and electron microscopy of compound eyes, adult heads were fixed, embedded in plastic, and sectioned as described previously (Van Vactor *et al*., 1991).

For quantification of Syntaxin16 localization imaginal discs expressing the indicated GFP-tagged transgenes were double-stained with anti-dSyx16 antibodies and anti-GFP antibodies. Individual image were captured by confocal microscopy. dSyx16-positive structures were counted as double positive if there was some overlap between GFP and dSyx16 staining, even if the centers of two stainings were offset.

RESULTS

Car *Is an Essential Gene*

To generate a null allele of *car*, we imprecisely excised the P(lacW)^{G0447} transposon inserted in its 5′ untranslated region (UTR). Among four mapped deletions, three extended into the neighboring gene *grip84*. One deletion, *car*$^{\Delta 146}$, eliminated almost the entire *car* coding unit (amino acids [aa] 1–584 of 617 aa) without disrupting neighboring genes (Figure 1B). Western blotting confirmed the loss of Car expression in the *car*$^{\Delta 146}$ allele (Figure 1C). Based on this molecular analysis, we consider *car*$^{\Delta 146}$ a null allele.

The *car*$^{\Delta 146}$ allele was hemizygous lethal; such larvae did not develop beyond the second instar, although *car*$^{\Delta 146}$ second instars could survive up to 6 d from the day of egg laying. Lethality caused by the *car*$^{\Delta 146}$ mutation was completely rescued by a transgene containing the genomic region of *car* (Figure 1B) or by a car cDNA under control of the ubiquitously expressed da-Gal4 driver (Wodarz *et al*., 1995). These results confirmed that the lethality of the *car*$^{\Delta 146}$ chromosome is due to the loss of *car* function.

Eyes in which subsets of cells lacked *car* function were generated using the FLP/FRT system (Xu and Rubin, 1993). Patches of homozygous *car*$^{\Delta 146}$ mutant cells in adult eyes lacked almost all pigmentation (Figure 1E) similar to cells carrying the strong *dor*^{8} allele (Figure 1F). This result is consistent with the *car*^{1} mutant phenotype and the requirement of the HOPS complex in trafficking to pigment granules during eye development (Warner *et al*., 1998; Sevrioukov *et al*., 1999; Pulipparacharuvil *et al*., 2005).

Loss of Function Causes Late Degeneration

Mosaic eyes containing *car*$^{\Delta 146}$ mutant and wild-type cells revealed additional functions of Car (Figure 2). In sections of eye from 2-d-old flies, patches of mutant cells were identified by their lack of pigmentation. In mutant ommatidia (red arrowhead in Figure 2A), all photoreceptors cells were present and arranged in their normal trapezoidal configuration. Because ommatidial development requires repeated cell–cell communication mediated by several signaling pathways, including Hedgehog, Notch, and receptor tyrosine kinase signaling (reviewed in Nagaraj and Banerjee, 2004; Silver and Rebay, 2005), our data indicate that *car* function is not strictly required for those signaling pathways in the developing eye.

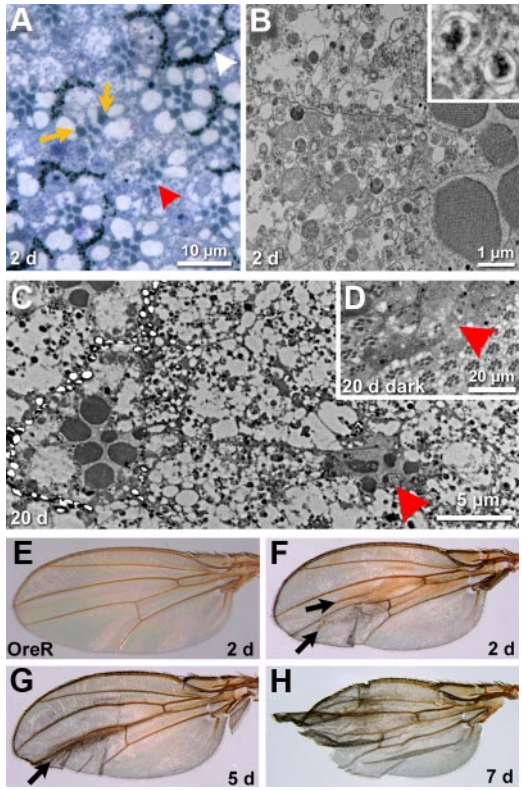

Figure 2. Loss of car causes late degeneration. (A) Micrograph of a section of a 2-d-old adult eye containing *car*$^{\Delta 146}$ mutant cells identified by the loss of pigmentation. The trapezoidal arrangement of rhabdomeres characteristic for wild-type ommatidia (white arrowhead) is not altered in the *car*$^{\Delta 146}$ommatidia (red arrowhead). Rhabdomeres of mutant cells are smaller. This phenotype is cell autonomous as in mixed ommatidia *car*$^{+}$ photoreceptor cells (recognized by their normal pigmentation, orange arrows) also have normal rhabdomere size but do not rescue neighboring *car*$^{\Delta 146}$ cells (identified by their lack of pigmentation in a w^{+} background. (B) An electron micrograph of a 2-d-old *car*$^{\Delta 146}$ ommatidium reveals the accumulation of vacuoles in the mutant photoreceptor cells, which nevertheless display well-organized rhabdomeres. The inset shows two examples in which the double membranes typical for autophagosomes are resolved. (C) Electron micrograph of a 20-d-old compound eye. A *car*$^{\Delta 146}$ ommatidium (red arrowhead) shows massive degeneration. (D) A micrograph depicts the eye of a fly raised for 20 d in the dark. Mutant ommatidia are degenerated (red arrowhead). (E–H) Wings from wild-type flies (E) or flies carrying *car*$^{\Delta 146}$ clones. Wing clones are not marked, but the majority of flies exhibiting *car*$^{\Delta 146}$ clones in the eye contained brown blemishes on the wings after just 2 to 5 d (arrows in F and G). Later, most of those wings became frail and damaged (H). Genotypes: w^{+} *car*$^{\Delta 146}$ FRT^{19A}/w^{+} FRT^{19A}; hsFLP (A–D and F–H) Oregon R (E).

Closer inspection revealed that rhabdomeres, although correctly positioned, were smaller in *car*$^{\Delta 146}$ photoreceptor cells of young adult flies (Figure 2A). This phenotype is cell-autonomous: rhabdomeres of individual *car*$^{+}$ cells seemed normal (see arrows in Figure 2A), even when surrounded by *car*$^{\Delta 146}$ cells. In addition, *car*$^{\Delta 146}$ photoreceptors had an extensive accumulation of vacuoles (Figure 2B). For many of these vacuoles, electron micrographs could resolve the double membranes typical for autophagosomes (see inset in Figure 2B for two examples). These data suggest that, similar to other HOPS subunits in *Drosophila* (Pulipparacharuvil *et al*., 2005; Lindmo *et al*., 2006) or yeast (Klionsky, 2005), Car is required for the fusion between lysosomes and

autophagosomes, and these normally transient structures accumulate in *car* null cells.

Defects in autophagy have been linked to neurodegeneration (Cuervo, 2006; Rubinsztein, 2006); therefore, we wanted to investigate the long-term consequences of loss of *car* function. In young flies, retinal cells were fully formed but 20-d-old flies exhibited extensive degeneration rendering most cellular structures, including rhabdomeres, barely recognizable (arrowhead in Figure 2C). Several forms of retinal degeneration are dependent on the activation of the phototransduction cascade (Wang and Montell, 2007). We therefore investigated eyes of flies that were raised for 20 d in the dark. In such dark-raised flies, $car^{\Delta 146}$ cells, nevertheless, exhibited massive degeneration (Figure 2D). Therefore, retinal degeneration in *car* null eyes was not light dependent.

Consistent with a mechanism independent of the phototransduction cascade, degeneration was not restricted to the eye but was also apparent in wings of flies with $car^{\Delta 146}$ clones. In young flies (2 d after eclosion), the first sign of this degeneration was a darkening of different wing areas (arrows in Figure 2, F and G). In older flies, the wings started to become frayed and ended up notched (Figure 2H). It is important to note that this age-dependent degeneration is mechanistically distinct from the "notched wing" phenotypes observed in mutants with partially inactivated Notch signaling which exhibit morphogenetic defects early during larval stages (Major and Irvine, 2005). Instead, this late phenotype is reminiscent of the wing blemishes observed in cell death mutants that interfere with posteclosion elimination of wing cells by the concerted activity of apoptosis and autophagy (Kimura *et al*., 2004; Link *et al*., 2007).

Car *Is Required for Endocytic Trafficking to Lysosomes*

To analyze whether *car* is required for endocytic trafficking we investigated several ligands and receptors in $car^{\Delta 146}$ cells in third instars. The Boss protein is expressed on the apical surface of developing R8 photoreceptors cells and its binding to the Sevenless receptor triggers Boss internalization into R7 precursor cells where it is degraded in <2 h (Krämer *et al*., 1991). In $car^{\Delta 146}$ ommatidia, Boss is still targeted to the apical domain of R8 cells. However, internalized Boss accumulates in $car^{\Delta 146}$ R7 cells beyond normal levels (Figure 3A). This suggested a defect in endocytic trafficking of Boss.

This defect is not specific for Boss, as several other ligands and receptors exhibited similar accumulation. For example, Delta accumulated in $car^{\Delta 146}$ cells (Figure 3, A and B). Furthermore, intracellular levels of Notch were elevated in patches of $car^{\Delta 146}$ cells (Figure 3C), whereas the level of Notch on the apical cell surface was not altered (arrows in Figure 3, C and C′). To test whether this effect is restricted to transmembrane proteins, we analyzed the distribution of Wingless (Wg) in wing discs with patches of $car^{\Delta 146}$ cells and found that this secreted ligand also accumulated in mutant cells (Figure 3E).

Among different ligands and receptors tested, the accumulation was most striking for Delta; therefore, we focused on the intensely stained Delta-positive compartments in $car^{\Delta 146}$ cells to further characterize the requirement for Car. First, we tested whether Delta accumulates within the secretory system. However, there was no significant overlap between the Golgi protein Lava lamp and Delta-positive compartments in $car^{\Delta 146}$ cells (Figure 3F). This result, together with the normal delivery of Boss and Notch to the apical surface (Figure 3, A and C), pointed to Delta accumulating in endosomal compartments. To directly test this possibility, we incubated live discs with antibodies against the extracellular domain of Delta (Le Borgne and Schweisguth, 2003). After a chase of 30 or 60 min, the extracellularly added antibodies were detected in the Delta-positive compartments in $car^{\Delta 146}$ cells, identifying them as part of the endocytic systems (Figure 3D and Supplemental Figure S1).

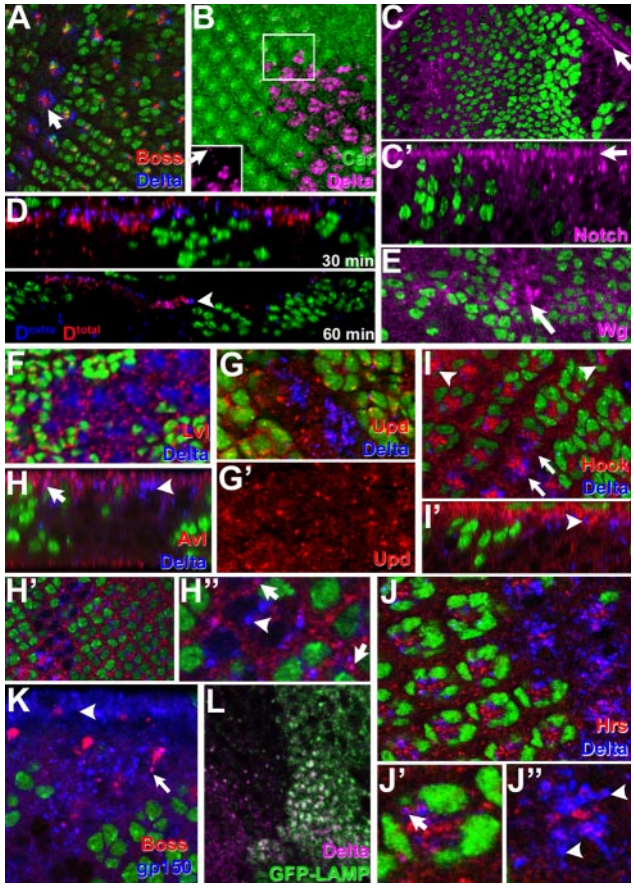

Figure 3. Car is required for normal trafficking of endocytosed proteins. In micrographs of parallel (A–C, E–K) or Z-sections (C′, D, H, and I′) the absence of the nuclear GFP marker (A, C–K) or Car staining (B) identified clones of $car^{\Delta 146}$ mutant cells in otherwise wild-type eye discs or wing discs (E). In $car^{\Delta 146}$ cells, Boss and Delta (A), Delta (B), Notch (C), and Wg (E) accumulated. The inset in B shows the Delta channel only to visualize the comparably low level of Delta in wild-type cells (arrow). Levels of apical cell surface Notch protein (arrows in C and C′) were not altered despite the intracellular accumulation. (D) Antibodies against the extracellular domain of Delta (D^{extra}) were internalized by live eye discs for the indicated time. Subsequently, discs were fixed, permeabilized and the location of internalized antibodies was compared with that of total Delta (D^{total}). The arrowhead points to examples of antibodies internalized into the large Delta-positive compartments in $car^{\Delta 146}$ clones. (F) Delta-positive compartments in $car^{\Delta 146}$ clones were negative for the Golgi marker Lvl. (G) Upd was not up-regulated in $car^{\Delta 146}$ clones. Large Delta-positive compartments in $car^{\Delta 146}$ clones (arrowheads in H–J) were negative for the endosomal markers Avl (H), Hook (I), and Hrs (J), but in wild-type and $car^{\Delta 146}$ mutant cells small apical Delta-positive vesicles were positive for these endosomal markers (arrows in H, H″, and J′). (K) The late endosomal protein gp150 colocalizes with Boss proteins endocytosed into $car^{\Delta 146}$ mutant R7 cells (arrow). (L) Delta-positive compartments were labeled by GFP-LAMP1, which accumulated in $car^{\Delta 146}$ cells. Genotypes: w^{1118} $car^{\Delta}146$ FRT^{19A}/w^{1118} P[w^{+},ubi>nGFP] FRT^{19A}; hsFLP (A–K).

Defects in several other endocytic trafficking mutants interfere with normal cell signaling (Seto *et al*., 2002). For

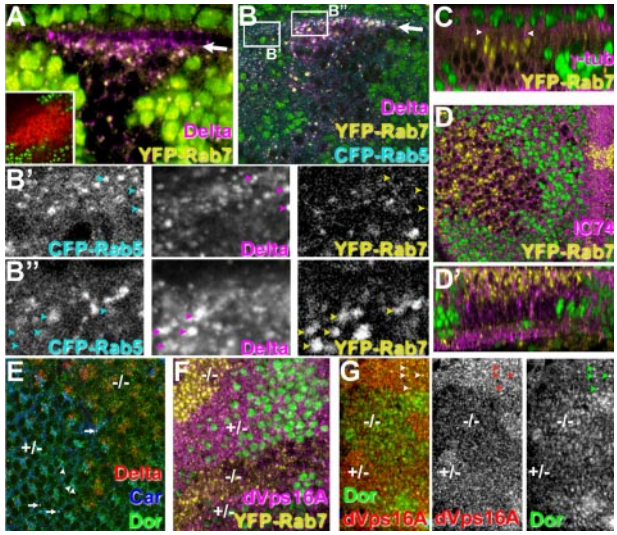

Figure 4. Loss of *car* function causes the accumulation of cargo in displaced Rab7-positive late endosomes. The absence of a nuclear GFP marker (green in A–D, F, and G) or Car staining (E) identified $car^{\Delta 146}$ cells in otherwise wild-type wing discs (A, B, F, and G) or eye discs (C–E). (A and B) Z-sections of imaginal discs taken at a slight angle revealed that in $car^{\Delta 146}$ mutant cells, Delta accumulated in YFP-Rab7–positive late endosomes, which were highly enriched just below the apical surface (arrows in A and B). The inset in A shows the accumulation of LysoTracker (red) in acidified endosomes of $car^{\Delta 146}$ mutant cells (marked by absence the nuclear GFP). Higher magnification of CFP-Rab5, Delta and YFP-Rab7 depict Delta in Rab5-positive early endosomes in wild-type cells (B′) but accumulated in Rab7-positive late endosomes in $car^{\Delta 146}$ mutant cells (B″). (C) YFP-Rab7–positive late endosomes are enriched close to centrosomes marked by γ-tubulin and are labeled by IC74 (D), which recognizes the dynein IC (D′ is a Z-section). (E) In wild-type cells (+/−), Car and Dor colocalize (examples labeled by arrowheads) and are found on some vesicles containing Delta (arrows). However, in $car^{\Delta 146}$ cells Dor is not reduced but does not label the large Delta-positive vesicles. (F) In $car^{\Delta 146}$ cells (−/−) with apical enriched YFP-Rab7 endosomes, apical dVps16A is reduced. (G) Dor and dVps16A colocalize in wild-type cells (arrowheads), but in $car^{\Delta 146}$ cells (−/−) dVps16A is reduced, whereas Dor seems enhanced. Genotypes: w^{1118} $car^{\Delta 146}$ FRT^{19A}/w^{1118} P[w^+,ubi>nGFP] FRT^{19A}; hsFLP; P[w^+ tub>YFP-Rab7] (A, C, D, and F); w^{1118} $car^{\Delta 146}$ FRT^{19A}/w^{1118} P[w^+,ubi>nGFP] FRT^{19A}; hsFLP; P[w^+ tub>YFP-Rab7] P[w^+ tub>CFP-Rab5] (B) w^{1118} $car^{\Delta 146}$ FRT^{19A}/w^{1118} FRT^{19A}; hsFLP (E) w^{1118} $car^{\Delta 146}$ FRT^{19A}/w^{1118} P[w^+,ubi>nGFP] FRT^{19A}; hsFLP (G).

example, in cells mutant for *erupted* or *dVps25* Notch signaling is activated and triggers the expression of Upd (Moberg *et al*., 2005; Thompson *et al*., 2005; Vaccari and Bilder, 2005; Herz *et al*., 2006). Unlike those mutants, $car^{\Delta 146}$ cells do not up-regulate Upd (Figure 3, G and G′), consistent with the normal formation of $car^{\Delta 146}$ ommatidia (Figure 2).

To further address the identity of the $car^{\Delta 146}$-induced Delta-positive compartments, we compared their distribution to a set of endocytic marker proteins. Avl, Hrs, and Rab5 are present on early endosomes (Lloyd *et al*., 2002; Wucherpfennig *et al*., 2003; Lu and Bilder, 2005). These markers colocalized with Delta in apical early endosomes of wild-type and $car^{\Delta 146}$ cells (arrows in Figure 3, H and J′), but the majority of the intensely stained Delta-positive compartments in $car^{\Delta 146}$ were negative for early endosomal markers (arrowheads in Figure 3, H, H″, and J″; also see Figure 4B). Similarly, Delta-positive compartments in $car^{\Delta 146}$ cells did not significantly colocalize with Hook (Figure 3I) or Rab11 (data not shown), a marker for recycling endosomes.

Significant labeling of Delta-positive compartments in $car^{\Delta 146}$ was observed with the late endosomal markers Rab7-YFP (Figure 4, A and B). Consistent with an accumulation in late endosomes, Gp150 a late endosomal protein implicated in Notch signaling (Li *et al*., 2003) colocalized with Boss endocytosed into $car^{\Delta 146}$ R7 cells (Figure 3K). Furthermore, the Delta-positive compartments were marked by GFP-LAMP1 (Figure 3L), which accumulated in $car^{\Delta 146}$ cells as reported previously for loss of dVps16A (Pulipparacharuvil *et al*., 2005). Together, these data demonstrate that, in the absence of *car* function, endocytosed ligands pass through early endosomes and accumulate in a Rab7-positive late endocytic compartment.

Late Endosomes Cluster in the Absence of Car

In wild-type imaginal disk cells, Rab5-CFP is present in early endosomes just below the apical surface, whereas Rab7-YFP is distributed throughout cells (Figure 4B; Marois *et al*., 2006). By contrast, in $car^{\Delta 146}$ cells Rab7-YFP is highly enriched in acidified Delta-positive compartments close to the subapical early endosomes marked by Rab5-CFP (Figure 4, A and B). Nevertheless, these clustered Rab7-positive late endosomes were not enriched in Rab5 (see arrowheads in Figure 4B″). Rab7-positive endosomes clustered close to the apically localized γ-tubulin (Figure 4C), reminiscent of the pericentriolar accumulation of late endosomes and lysosomes after overexpression of mVps18, mVps33B, or hVps39 (Caplan *et al*., 2001; Poupon *et al*., 2003; Gissen *et al*., 2005).

We therefore wondered whether the accumulation of Rab7-positive endosomes correlated with an increased recruitment of subunits of the HOPS complex. In wild-type cells, Dor is detected in a punctate pattern, partially colocalizing with Car (e.g., arrowheads in Figure 4E) and a subset of these punctae are positive for Delta, indicating they represent endosomes (arrows in Figure 4E). In $car^{\Delta 146}$ cells, Dor was still present in a punctate pattern and, at levels just below the apical surface, Dor seemed slightly enriched in $car^{\Delta 146}$ cells (Figure 4, G and G′).

The opposite was the case for dVps16A, which directly binds to Car (Pulipparacharuvil *et al*., 2005). In wild-type cells, dVps16A was apically enriched (Figure 4F) and colocalized with Dor (arrowheads in Figure 4G). By contrast, staining for dVps16A was markedly reduced in $car^{\Delta 146}$ cells, despite the accumulation of Rab7-positive vesicles (Figure 4F). The differential response of Dor and dVps16A to the loss of Car protein was most obvious in their direct comparison, where $car^{\Delta 146}$ cells exhibited reduced dVps16A staining while simultaneously enhanced Dor staining was apparent in optical sections just below the apical surface (Figure 4G). These results are consistent with the idea that a direct interaction with Car is critical for the recruitment of dVps16A but not Dor to endosomes.

An alternative mechanism for the clustering of late endosomes was suggested by observations in mammalian cells where Rab7-GTP can recruit the Dynein/Dynactin receptors RILP and ORPIL to late endosomes, thus triggering their movement toward the minus ends of microtubules at centrosomes (Jordens *et al*., 2001; Johansson *et al*., 2007). Consistent with this possibility, we found dynein light chain present at Rab7-positive endosomes in $car^{\Delta 146}$ cells (Figure 4, D and D′).

Car *binds to dSyntaxin 16*

A key function of SM proteins like Car is their binding to syntaxins (Rizo and Sudhof, 2002; Jahn and Scheller, 2006). To test different *Drosophila* homologues of syntaxins that act

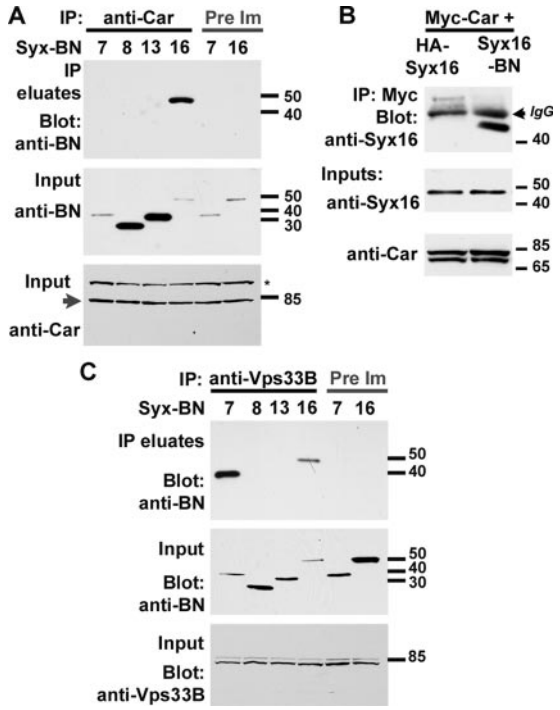

Figure 5. Car binds to dSyntaxin16. Car (A and B) or dVps33B (C) were coexpressed in S2 cells with the indicated Syntaxins carrying a C-terminal BN epitope-tag replacing the transmembrane domain or an N-terminal HA-tag in (B). Expression levels were detected on blots of input samples by using the indicated antibodies. Protein complexes were immunoprecipitated with anti-Car (A), anti-Myc (B), or anti-dVps33B (C) antibodies or preimmunsera when indicated. Coimmunoprecipitated syntaxins were detected using the anti-BN antibodies (A and C) or anti-dSyntaxin16 (B). Note that dSyntaxin7 is synonymous with Avl.

in endosomal pathways (Hong, 2005) for possible interactions with Car, we used coimmunoprecipitation experiments. Car, or its closest homologue dVps33B, was coexpressed in S2 cells together with different syntaxins in which the C-terminal transmembrane domain had been replaced by an epitope tag. Coimmunoprecipitation using anti-Car antibodies, but not preimmune sera, specifically pulled down dSyntaxin16 (Figure 5A).

It is interesting to note that this interaction was not observed when N-terminally tagged Syntaxins were used for pull-down (Figure 5B). This suggests that the binding of Car to dSyntaxin16 involves the N-terminal region of dSyntaxin16, similar to interactions between other Syntaxins and SM proteins (Dulubova *et al*., 2002; Hu *et al*., 2007).

Binding of Car to dSyntaxin16 was surprising, because it had been localized previously to the Golgi complex (Xu *et al*., 2002). However, only a subset of dSyntaxin16 colocalized with Golgi markers in salivary glands (Xu *et al*., 2002) or eye discs (Figure 6A). The remaining Syx16 was mostly present on lysosomes as 71% of LAMP-GFP overlapped with Syx16-positive structures (Figure 6, B and G; 71 ± 13%, n = 494 in 8 imaginal discs). Late endosomes marked by YFP-Rab7 exhibited less overlap (Figure 6, C and G; 45 ± 11%, n = 535 in 10 discs). By contrast, overlap with the early endosome marker CFP-Rab5 was minimal (Figure 6, D and G; 19 ± 5%, n = 1179 in 7 discs). Further support for a role of dSyntaxin16 in lysosomes came from its altered distribution in $car^{\Delta 146}$ cells; whereas in neighboring wild-type cells some vesicles were double positive for YFP-Rab7 and dSyntaxin16

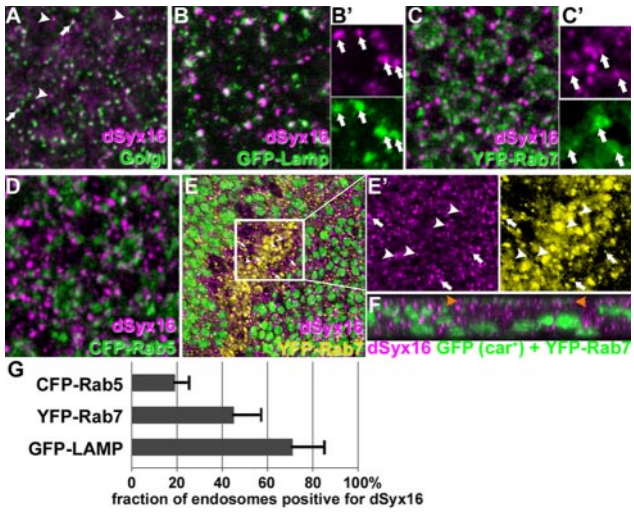

Figure 6. dSyntaxin16 is present in Golgi and lysosomes. Micrographs of eye discs visualize dSyntaxin16 and markers for the Golgi complex (A; 7H6D7C2), lysosomes (B; GFP-Lamp), late endosomes (C; YFP-Rab7), and early endosomes (D; CFP-Rab5). Although dSyntaxin16 extensively colocalized with the Golgi marker (arrows in A) a subset of dSyntaxin16-positive punctae is negative for 7H6D7C2 staining (arrowheads in A). Some dSyntaxin16-positive punctae colocalized with GFP-Lamp (arrows in B′) or YFP-Rab7 (arrows in C′) but rarely CFP-Rab5 (D). In $car^{\Delta 146}$ mutant cells, YFP-Rab7-positive late endosomes were enriched but negative for dSyntaxin16 (E and F). Higher magnifications micrographs depict the colocalization of YFP-Rab7 and dSyntxin16 in neighboring wild-type cells (arrows in E′) but in $car^{\Delta 146}$ cells the few strongly stained dSyntaxin16 punctae were negative for YFP-Rab7 (arrowheads in E′). The Z-section depicted in F shows a $car^{\Delta 146}$ clone. Between the arrowheads apically accumulated YFP-Rab7 is shown in green. (G) Quantification of the fraction of Rab5-marked early endosomes, Rab7-marked late endosomes or Lamp-marked lysosomes that were also stained for endogenous dSyx16. Genotypes: OreR (A) $w^{1118;}$ [w^{+},tub>GFP-LAMP] (B) $w^{1118;}$ [w^{+},tub>YFP-Rab7] (C) $w^{1118;}$ [w^{+},tub>CFP-Rab5] (D) w^{1118} $car^{\Delta 146}$ FRT^{19A}/w^{1118} P[w^{+},ubi>nGFP] FRT^{19A}; hsFLP; P[w^{+} tub>YFP-Rab7] (E).

(arrows in Figure 6, E and E′), dSyntaxin16 did not localize to the enlarged YFP-Rab7 positive late endosomes in $car^{\Delta 146}$ cells (Figure 6E, white arrowheads; and F). These data suggest that dSyntaxin16 may be present on lysosomes—rather than YFP-Rab7 positive late endosomes—during the fusion reaction and that it is likely to be delivered there by a route distinct from Rab7-positive late endosomes.

Car *and dVps33B Are Not Redundant*

We also examined the binding of Car's closest *Drosophila* homologue dVps33B to endocytic syntaxins. After coexpression in S2 cells, dVps33B bound most strongly to Avl, a syntaxin implicated in early endosomal fusions (Lu and Bilder, 2005). A weaker interaction was also observed with dSyntaxin16 but not dSyntaxin13 or dSyntaxin8 (Figure 5C).

Although binding of dVps33B to dSyntaxin16 was weak compared with Avl, it raised the possibility that dVps33B might be able to partially substitute for Car. To explore this possibility, we generated transgenic flies expressing dVps33B under UAS control (Figure 7A). Overexpression of this transgene under the control of several drivers (da-, act-, or arm-Gal4) did not elicit phenotypic responses in wild-type flies. Using the MARCM system (Lee and Luo, 2001), we specifically expressed dVps33B in $car^{\Delta 146}$ cells. Expression of dVps33B was not able to restore pigmentation in

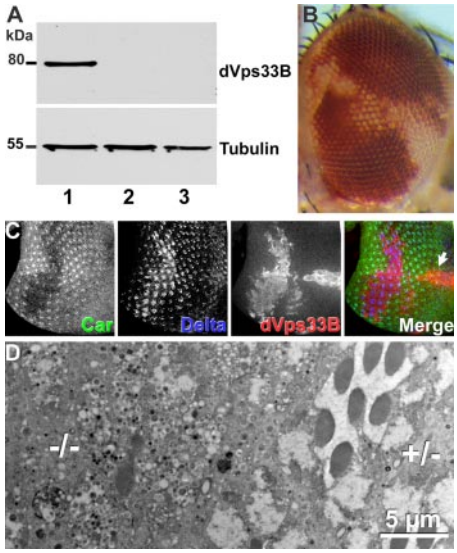

Figure 7. dVps33B cannot replace Car. (A) Western blots of lysates from fly heads with the genotypes (1) $car^{\Delta 146}$ FRT19A/tub-Gal80 FRT19A; tub-Gal4; UAS-Myc-dVps33B (2) UAS-Myc-dVps33B (3) $car^{\Delta 146}$ FRT19A/tub-Gal80 FRT19A; tub-Gal4 show the expression of Myc-dVps33B in MARCM clones (Lee and Luo, 2001). (B) Micrograph of an adult eye expressing *dVps33B* by using the MARCM technique, which did not restore pigmentation in $car^{\Delta 146}$ mutant cells. (C) Expression of *dVps33B* in a $car^{\Delta 146}$ clone did not restore normal trafficking of Delta in a third instar eye disk. (D) An electron micrograph of a section of an adult eye shows that dVps33B expression did not prevent degeneration of $car^{\Delta 146}$ cells. Genotypes: w^{+} $car^{\Delta 146}$ FRT^{19A}/w^{1118} P[*w*+ tubP>GAL80] hsFLP, FRT^{19A}; P[*w*+ tubP>Gal4]/+; P[*w*+ UAS-Myc-dVps33B]/+ (B–D).

clones of $car^{\Delta 146}$ cells in the adult eye (Figure 7B), or restore normal trafficking of Delta to lysosomes in $car^{\Delta 146}$ cells in imaginal discs (Figure 7C). Furthermore, the late degeneration in patches of $car^{\Delta 146}$ cells in the eye was not prevented by dVps33B expression (Figure 7D). Together, these results argue against the possibility that dVps33B can act redundantly with Car and usurp its function in the HOPS complex. Thus, Car is the major SM protein necessary for trafficking to pigment granules and is also required for endosomal and autophagosomal cargo to reach lysosomes.

DISCUSSION

Car/*Vps33A Is the Principle SM Protein Required for Membrane Fusions of Lysosomes and LROs*

Three SM proteins have been implicated in membrane fusion events in the endocytic pathway: Vps45, Vps33B, and Car/Vps33A. Our analysis of a *car* null allele indicates that Car is the major SM protein required for the delivery of endosomal content to lysosomes in *Drosophila*. Furthermore, Car is required for the biogenesis of pigment granules, the only lysosome-related organelle so far described in *Drosophila* (Lloyd *et al*., 1998). These requirements are consistent with the presence of Car in a complex with other Vps-C proteins, its binding to dVps16A (Sevrioukov *et al*., 1999; Pulipparacharuvil *et al*., 2005), and the subtle trafficking defects observed in the mild car^{1} allele (Sriram *et al*., 2003). Consistent with the observations of Sriram *et al*. (2003), our data also point to distinct functions for different Vps-C proteins, because endosomes in *car* mutant cells exhibit reduced dVps16A but increased Dor levels. Whether Car contributes to the dissociation of Dor via catalyzing the fusion reaction itself or by a distinct mechanism is not clear yet.

Car *and Degeneration*

One important consequence of loss of *car* function was the degeneration of photoreceptor neurons (Figure 2). Neurodegeneration is a common consequence of lysosomal dysfunction, examples include different forms of neuronal ceroid lipofuscinoses in humans (Haltia, 2003), loss of the major lysosomal protease cathepsin D in mice (Shacka *et al*., 2007) or mutations in the lysosomal sugar transporter Benchwarmer/Spinster in *Drosophila* (Dermaut *et al*., 2005). Compared with *benchwarmer/spinster* in which inclusions of abnormal late endosomes and lysosomes accumulate, the late degeneration of *car* null cells is substantially more severe: in 20-d-old photoreceptors, cellular content was no longer recognizable (Figure 2).

The consequences of lysosomal dysfunction are likely to be further enhanced by the loss of fusion with autophagosomes. The HOPS complex is necessary for fusion of autophagosomes with vacuoles in yeast (Klionsky, 2005), and this function is conserved as loss-of-function phenotypes of *dor*, *dVps16A* and *car* all include the accumulation of autophagosomes (Figure 2; Pulipparacharuvil *et al*., 2005; Lindmo *et al*., 2006) and further enhance such phenotypes in the *bluecheese* mutant (Simonsen *et al*., 2007). Impaired autophagy in itself can be sufficient to trigger neurodegeneration as brain-specific knockouts of Atg5 and Atg7 demonstrated (Hara *et al*., 2006; Komatsu *et al*., 2006). Thus, the severity of the *car* null degeneration phenotype is consistent with its dual function in the fusion of lysosomes with late endosomes and autophagosomes.

Car *Interacts with dSyntaxin16*

A general function of SM proteins is their binding to syntaxins (Hata *et al*., 1993). We were surprised to find that, in vitro, Car binds to dSyntaxin16, which has previously been described for its function in the Golgi complex (Xu *et al*., 2002). Interestingly, those authors observed that only a subset of Syntaxin16 localized to the Golgi complex, whereas a smaller fraction was present at organelles not further characterized. Our data identify a fraction of the dSyntaxin16-positive structures as lysosomes (Figure 6). Experiments testing possible genetic interactions between *car* and *dSyx16* are hampered by the lack of dSyx16 mutants or efficient RNAi trangenes and the proximity of the two genes on the x-chromosome. However, participation of dSyntaxin16 in two distinct fusion events in the secretory and the endosomal pathway is not without precedent among SNARE proteins; other examples include soluble *N*-ethylmaleimide-sensitive factor attachment protein-25 (Aikawa *et al*., 2006) and Synaptobrevin (Deak *et al*., 2004).

How dSyntaxin16 is targeted to these different membranes is not clear. During vacuolar fusion in yeast, Vps33 interacts with the syntaxin Vam3 (Dulubova *et al*., 2001) which is delivered from the Golgi complex to the vacuole via the adaptor protein-3 (AP-3)–dependent pathway (Cowles *et al*., 1997). This may also be the case for the lysosomal subset of dSyntaxin16, because its absence from the Rab7-positive compartment in *car* null cells (Figure 6) argues against a delivery via the late endosomal route. Consistent with an AP-3–dependent pathway to lysosomes is the genetic interaction between *garnet* and *car* (Lloyd *et al*., 1998). The *garnet* eye color mutant encodes the δ subunit of the AP-3 complex and the mild phenotypes observed in *garnet* (Ooi *et al*., 1997; Simpson *et al*., 1997; Lloyd *et al*., 1999) and mutations in other AP-3 subunits (Boehm and Bonifacino,

2001) suggest that the AP-3 pathway to lysosomes can be partially supplanted by the endosomal route. Such a salvage pathway to lysosomes explained the subtle changes in human cells deficient for the β3A subunit (Dell'Angelica *et al*., 1999). Reduced activity of this salvage pathway in the mild car^1 allele thus could explain the genetic interaction between the *garnet* and *car* mutants.

A Function of Car *in Early Endosomes?*

Vps33p, as part of the class C Vps complex, is also required during fusion events with early endosome membranes in yeast (Peterson and Emr, 2001; Subramanian *et al*., 2004). In *Drosophila*, we found no evidence for such a role of Car. Our data indicate that *car* null cells internalized ligands, which moved through early endosomes marked by Avl, Hrs, and Rab5 to eventually accumulate in a Rab7-positive late endosomal compartment (Figures 3 and 4).

The accumulation of ligands and receptors in $car^{\Delta 146}$ cells is not accompanied by ectopic signaling. By contrast, interference with early endosome fusions by mutations in the syntaxin Avl or the GTPase Rab5 result in severe developmental defects due to the accumulation of the Notch receptor and the apical determinant Crumbs (Lu and Bilder, 2005). Similarly, developmental defects result from the inactivation of *Drosophila* homologues of class E *vps* genes (Moberg *et al*., 2005; Sevrioukov *et al*., 2005; Thompson *et al*., 2005; Vaccari and Bilder, 2005; Herz *et al*., 2006). This subset of vps genes, including *vps23*, *vps25*, and *vps28*, have been implicated in the sorting of cargo into multivesicular bodies (MVBs) in yeast and metazoa (Katzmann *et al*., 2002). Thus, the absence of cell fate changes in *car* mutant cells despite the dramatic accumulation of ligands and receptors argues for a specific function of Car late in endocytic trafficking after the signaling of receptors is terminated by their sequestration into MVBs.

A possible explanation for our finding that Car, unlike yeast Vps33p, is dispensable for early endosomal fusions is the presence of Vps33B, a second Vps33 homologue in metazoa (Pevsner *et al*., 1996). A possible role of Vps33B in some early endosomal fusions is consistent with its binding to the early endosomal syntaxin Avl (labeled Syx7 in Figure 5). The consequences of the loss of Vps33B function are, however, not consistent with a complete loss of early endosomal fusions (Gissen *et al*., 2004; Matthews *et al*., 2005). This suggests an additional role for either Vps45 (Cowles *et al*., 1994; Piper *et al*., 1994; Morrison *et al*., 2008) or Vps33A in early endosome fusion events.

Recent studies described efficient clustering of LROs, including lysosomes and melanosomes close to the microtubule-organizing center (MTOC) in response to the overexpression of mammalian homologues of HOPS subunits (Caplan *et al*., 2001; Poupon *et al*., 2003; Gissen *et al*., 2005). These observations were interpreted as a reflection of HOPS-mediated tethering of LROs. Our findings suggest an alternative explanation for these results. In *car* null cells, we observed similar clustering of Rab7-positive late endosomes close to the microtubule-organizing center (Figure 4C). This may be a consequence of misregulated Rab7 activity, because in yeast the HOPS complex directly binds to Ypt7 and acts as its exchange factor (Seals *et al*., 2000; Wurmser *et al*., 2000). Misregulation of Rab7 can induce the dynein-mediated transport of late endosomes toward the MTOC (Jordens *et al*., 2001; Johansson *et al*., 2007). Thus, the pericentrosomal clustering of late endosomes/lysosomes after overexpression of HOPS subunits may not represent a HOPS gain-of-function phenotype in tethering, but a loss-of-function phenotype, a common consequence when individual subunits of multiprotein complexes are overexpressed (Herskowitz, 1987).

A function in endosome maturation has recently been proposed for HOPS-like complexes based on observations that such complexes, including hVps16 and hVps18 catalyze the exchange of Rab5 to Rab7 (Rink *et al*., 2005). Similarly in yeast, the exchange of Vps21p to Ypt7p may be associated with the transformation of the CORVET to the HOPS complex, which both share Vps33p as part of the Vps-C core (Peplowska *et al*., 2007). Car/Vps33A is not required for Rab5/7 conversion during endosome maturation in *Drosophila*, as in $car^{\Delta 146}$ imaginal cells internalized ligands accumulated in a Rab5-negative/Rab7-positive compartment (Figure 4). Instead, this role may be filled by Vps33B. Null mutations in the two Vps33 homologues in the same model system will be necessary to fully understand the level to which these proteins have overlapping and distinct functions.

ACKNOWLEDGMENTS

We thank Ege Kavalali and Adam Haberman for critical reading of the manuscript. We are grateful to Mary Kuhn for technical assistance. We thank the Bloomington Stock Center for fly stocks and the Developmental Studies Hybridoma Bank (University of Iowa, Iowa City, IA) for antibodies. We thank Hugo Bellen (Baylor College of Medicine, Houston, TX), Marc Muskavitch (Boston College, Boston, MA), Nick Baker (Albert Einstein College of Medicine, Bronx, NY), William Trimble (Hospital for Sick Children, Toronto), Susan Eaton (MPI, Dresden, Germany), and Zhi-Chun Lai (Pennsylvania State University, University Park, PA) for antibodies and fly lines. This work was supported by The Welch Foundation grant I-1300 and National Institutes of Health grant EY10199.

REFERENCES

Aikawa, Y., Lynch, K. L., Boswell, K. L., and Martin, T. F. (2006). A second SNARE role for exocytic SNAP25 in endosome fusion. Mol. Biol. Cell *17*, 2113–2124.

Banta, L. M., Vida, T. A., Herman, P. K., and Emr, S. D. (1990). Characterization of yeast Vps33p, a protein required for vacuolar protein sorting and vacuole biogenesis. Mol. Cell Biol. *10*, 4638–4649.

Beadle, G. W., and Ephrussi, B. (1936). The differentiation of eye pigments in *Drosophila* as studied by transplantation. Genetics *21*, 225–247.

Bethani, I., Lang, T., Geumann, U., Sieber, J. J., Jahn, R., and Rizzoli, S. O. (2007). The specificity of SNARE pairing in biological membranes is mediated by both proof-reading and spatial segregation. EMBO J. *26*, 3981–3992.

Boehm, M., and Bonifacino, J. S. (2001). Adaptins: the final recount. Mol. Biol. Cell *12*, 2907–2920.

Brand, A. H., and Perrimon, N. (1993). Targeted gene expression as a means of altering cell fates and generating dominant phenotypes. Development *118*, 401–415.

Brenner, S. (1974). The genetics of *Caenorhabditis elegans*. Genetics *77*, 71–94.

Bunch, T. A., Grinblat, Y., and Goldstein, L. S. (1988). Characterization and use of the *Drosophila* metallothionein promoter in cultured *Drosophila* melanogaster cells. Nucleic Acids Res. *16*, 1043–1061.

Cai, H., Reinisch, K., and Ferro-Novick, S. (2007). Coats, tethers, Rabs, and SNAREs work together to mediate the intracellular destination of a transport vesicle. Dev. Cell *12*, 671–682.

Caplan, S., Hartnell, L. M., Aguilar, R. C., Naslavsky, N., and Bonifacino, J. S. (2001). Human Vam6p promotes lysosome clustering and fusion in vivo. J. Cell Biol. *154*, 109–122.

Carpp, L. N., Ciufo, L. F., Shanks, S. G., Boyd, A., and Bryant, N. J. (2006). The Sec1p/Munc18 protein Vps45p binds its cognate SNARE proteins via two distinct modes. J. Cell Biol. *173*, 927–936.

Casso, D., Ramirez-Weber, F., and Kornberg, T. B. (2000). GFP-tagged balancer chromosomes for *Drosophila melanogaster*. Mech. Dev. *91*, 451–454.

Cowles, C. R., Emr, S. D., and Horazdovsky, B. F. (1994). Mutations in the VPS45 gene, a SEC1 homologue, result in vacuolar protein sorting defects and accumulation of membrane vesicles. J. Cell Sci. *107*, 3449–3459.

Cowles, C. R., Odorizzi, G., Payne, G. S., and Emr, S. D. (1997). The AP-3 adaptor complex is essential for cargo-selective transport to the yeast vacuole. Cell *91*, 109–118.

Cuervo, A. M. (2006). Autophagy in neurons: it is not all about food. Trends Mol. Med. *12*, 461–464.

Deak, F., Schoch, S., Liu, X., Sudhof, T. C., and Kavalali, E. T. (2004). Synaptobrevin is essential for fast synaptic-vesicle endocytosis. Nat. Cell Biol. *6*, 1102–1108.

Dell'Angelica, E. C., Shotelersuk, V., Aguilar, R. C., Gahl, W. A., and Bonifacino, J. S. (1999). Altered trafficking of lysosomal proteins in Hermansky-Pudlak syndrome due to mutations in the beta 3A subunit of the AP-3 adaptor. Mol. Cell *3*, 11–21.

Dermaut, B., Norga, K. K., Kania, A., Verstreken, P., Pan, H., Zhou, Y., Callaerts, P., and Bellen, H. J. (2005). Aberrant lysosomal carbohydrate storage accompanies endocytic defects and neurodegeneration in *Drosophila* benchwarmer. J. Cell Biol. *170*, 127–139.

Dulubova, I., Khvotchev, M., Liu, S., Huryeva, I., Sudhof, T. C., and Rizo, J. (2007). Munc18–1 binds directly to the neuronal SNARE complex. Proc. Natl. Acad. Sci. USA *104*, 2697–2702.

Dulubova, I., Yamaguchi, T., Gao, Y., Min, S. W., Huryeva, I., Sudhof, T. C., and Rizo, J. (2002). How Tlg2p/syntaxin 16 'snares' Vps45. EMBO J. *21*, 3620–3631.

Dulubova, I., Yamaguchi, T., Wang, Y., Sudhof, T. C., and Rizo, J. (2001). Vam3p structure reveals conserved and divergent properties of syntaxins. Nat. Struct. Biol. *8*, 258–264.

Fehon, R. G., Kooh, P. J., Rebay, I., Regan, C. L., Xu, T., Muskavitch, M. A., and Artavanis-Tsakonas, S. (1990). Molecular interactions between the protein products of the neurogenic loci Notch and Delta, two EGF-homologous genes in *Drosophila*. Cell *61*, 523–534.

Gissen, P., Johnson, C. A., Gentle, D., Hurst, L. D., Doherty, A. J., O'Kane, C. J., Kelly, D. A., and Maher, E. R. (2005). Comparative evolutionary analysis of VPS33 homologues: genetic and functional insights. Hum. Mol. Genet. *14*, 1261–1270.

Gissen, P., *et al*. (2004). Mutations in VPS33B, encoding a regulator of SNARE-dependent membrane fusion, cause arthrogryposis-renal dysfunction-cholestasis (ARC) syndrome. Nat. Genet. *36*, 400–404.

Haltia, M. (2003). The neuronal ceroid-lipofuscinoses. J. Neuropathol. Exp. Neurol. *62*, 1–13.

Hara, T., *et al*. (2006). Suppression of basal autophagy in neural cells causes neurodegenerative disease in mice. Nature *441*, 885–889.

Hata, Y., Slaughter, C. A., and Sudhof, T. C. (1993). Synaptic vesicle fusion complex contains unc-18 homologue bound to syntaxin. Nature *366*, 347–351.

Hay, B. A., Wolff, T., and Rubin, G. M. (1994). Expression of baculovirus P35 prevents cell death in *Drosophila*. Development *120*, 2121–2129.

Hazelett, D. J., Bourouis, M., Walldorf, U., and Treisman, J. E. (1998). decapentaplegic and wingless are regulated by eyes absent and eyegone and interact to direct the pattern of retinal differentiation in the eye disc. Development *125*, 3741–3751.

Herskowitz, I. (1987). Functional inactivation of genes by dominant negative mutations. Nature *329*, 219–222.

Herz, H. M., Chen, Z., Scherr, H., Lackey, M., Bolduc, C., and Bergmann, A. (2006). vps25 mosaics display non-autonomous cell survival and overgrowth, and autonomous apoptosis. Development *133*, 1871–1880.

Hong, W. (2005). SNAREs and traffic. Biochim. Biophys. Acta *1744*, 493–517.

Hu, S. H., Latham, C. F., Gee, C. L., James, D. E., and Martin, J. L. (2007). Structure of the Munc18c/Syntaxin4 N-peptide complex defines universal features of the N-peptide binding mode of Sec1/Munc18 proteins. Proc. Natl. Acad. Sci. USA *104*, 8773–8778.

Jahn, R., Lang, T., and Sudhof, T. C. (2003). Membrane fusion. Cell *112*, 519–533.

Jahn, R., and Scheller, R. H. (2006). SNAREs—engines for membrane fusion. Nat. Rev. Mol. Cell Biol. *7*, 631–643.

Johansson, M., Rocha, N., Zwart, W., Jordens, I., Janssen, L., Kuijl, C., Olkkonen, V. M., and Neefjes, J. (2007). Activation of endosomal dynein motors by stepwise assembly of Rab7-RILP-p150Glued, ORP1L, and the receptor betaIII spectrin. J. Cell Biol. *176*, 459–471.

Jordens, I., Fernandez-Borja, M., Marsman, M., Dusseljee, S., Janssen, L., Calafat, J., Janssen, H., Wubbolts, R., and Neefjes, J. (2001). The Rab7 effector protein RILP controls lysosomal transport by inducing the recruitment of dynein-dynactin motors. Curr. Biol. *11*, 1680–1685.

Katzmann, D. J., Odorizzi, G., and Emr, S. D. (2002). Receptor downregulation and multivesicular-body sorting. Nat. Rev. Mol. Cell Biol. *3*, 893–905.

Kim, B. Y., Krämer, H., Yamamoto, A., Kominami, E., Kohsaka, S., and Akazawa, C. (2001). Molecular characterization of mammalian homologues of class C Vps proteins that interact with syntaxin-7. J. Biol. Chem. *276*, 29393–29402.

Kimura, K., Kodama, A., Hayasaka, Y., and Ohta, T. (2004). Activation of the cAMP/PKA signaling pathway is required for post-ecdysial cell death in wing epidermal cells of *Drosophila melanogaster*. Development *131*, 1597–1606.

Klionsky, D. J. (2005). The molecular machinery of autophagy: unanswered questions. J. Cell Sci. *118*, 7–18.

Komatsu, M., *et al*. (2006). Loss of autophagy in the central nervous system causes neurodegeneration in mice. Nature *441*, 880–884.

Krämer, H., Cagan, R. L., and Zipursky, S. L. (1991). Interaction of bride of sevenless membrane-bound ligand and the sevenless tyrosine-kinase receptor. Nature *352*, 207–212.

Krämer, H., and Phistry, M. (1996). Mutations in the *Drosophila hook* gene inhibit endocytosis of the boss transmembrane ligand into multivesicular bodies. J. Cell Biol. *133*, 1205–1215.

Latham, C. F., *et al*. (2006). Molecular dissection of the Munc18c/syntaxin4 interaction: implications for regulation of membrane trafficking. Traffic *7*, 1408–1419.

Le Borgne, R., and Schweisguth, F. (2003). Unequal segregation of Neuralized biases Notch activation during asymmetric cell division. Dev. Cell *5*, 139–148.

Lee, T., and Luo, L. (2001). Mosaic analysis with a repressible cell marker (MARCM) for *Drosophila* neural development. Trends Neurosci. *24*, 251–254.

Li, Y., Fetchko, M., Lai, Z. C., and Baker, N. E. (2003). Scabrous and Gp150 are endosomal proteins that regulate Notch activity. Development *130*, 2819–2827.

Lindmo, K., Simonsen, A., Brech, A., Finley, K., Rusten, T. E., and Stenmark, H. (2006). A dual function for Deep orange in programmed autophagy in the *Drosophila melanogaster* fat body. Exp. Cell Res. *312*, 2018–2027.

Link, N., Chen, P., Lu, W. J., Pogue, K., Chuong, A., Mata, M., Checketts, J., and Abrams, J. M. (2007). A collective form of cell death requires homeodomain interacting protein kinase. J. Cell Biol. *178*, 567–574.

Lloyd, T. E., Atkinson, R., Wu, M. N., Zhou, Y., Pennetta, G., and Bellen, H. J. (2002). Hrs regulates endosome membrane invagination and tyrosine kinase receptor signaling in *Drosophila*. Cell *108*, 261–269.

Lloyd, V., Ramaswami, M., and Krämer, H. (1998). Not just pretty eyes: *Drosophila* eye-colour mutations and lysosomal delivery. Trends Cell Biol. *8*, 257–259.

Lloyd, V. K., Sinclair, D. A., Wennberg, R., Warner, T. S., Honda, B. M., and Grigliatti, T. A. (1999). A genetic and molecular characterization of the *garnet* gene of *Drosophila melanogaster*. Genome *42*, 1183–1193.

Lu, H., and Bilder, D. (2005). Endocytic control of epithelial polarity and proliferation in *Drosophila*. Nat. Cell Biol. *7*, 1132–1139.

Major, R. J., and Irvine, K. D. (2005). Influence of Notch on dorsoventral compartmentalization and actin organization in the *Drosophila* wing. Development *132*, 3823–3833.

Marois, E., Mahmoud, A., and Eaton, S. (2006). The endocytic pathway and formation of the Wingless morphogen gradient. Development *133*, 307–317.

Matthews, R. P., Plumb-Rudewiez, N., Lorent, K., Gissen, P., Johnson, C. A., Lemaigre, F., and Pack, M. (2005). Zebrafish vps33b, an ortholog of the gene responsible for human arthrogryposis-renal dysfunction-cholestasis syndrome, regulates biliary development downstream of the onecut transcription factor hnf6. Development *132*, 5295–5306.

McNew, J. A., Parlati, F., Fukuda, R., Johnston, R. J., Paz, K., Paumet, F., Sollner, T. H., and Rothman, J. E. (2000). Compartmental specificity of cellular membrane fusion encoded in SNARE proteins. Nature *407*, 153–159.

Moberg, K. H., Schelble, S., Burdick, S. K., and Hariharan, I. K. (2005). Mutations in erupted, the *Drosophila* ortholog of mammalian tumor susceptibility gene 101, elicit non-cell-autonomous overgrowth. Dev. Cell *9*, 699–710.

Morrison, H. A., Dionne, H., Rusten, T. E., Brech, A., Fisher, W. W., Pfeiffer, B. D., Celniker, S. E., Stenmark, H., and Bilder, D. (2008). Regulation of early endosomal entry by the *Drosophila* tumor suppressors rabenosyn and Vps45. Mol. Biol. Cell *19*, 4167–4176.

Nagaraj, R., and Banerjee, U. (2004). The little R cell that could. Int. J. Dev. Biol. *48*, 755–760.

Novick, P., and Schekman, R. (1979). Secretion and cell-surface growth are blocked in a temperature-sensitive mutant of *Saccharomyces cerevisiae*. Proc. Natl. Acad. Sci. USA *76*, 1858–1862.

O'Neill, E. M., Rebay, I., Tjian, R., and Rubin, G. M. (1994). The activities of two Ets-related transcription factors required for *Drosophila* eye development are modulated by the Ras/MAPK pathway. Cell *78*, 137–147.

Ooi, C. E., Moreira, J. E., Dell'Angelica, E. C., Poy, G., Wassarman, D. A., and Bonifacino, J. S. (1997). Altered expression of a novel adaptin leads to defective pigment granule biogenesis in the *Drosophila* eye color mutant *garnet*. EMBO J. *16*, 4508–4518.

Parks, A. L., Turner, F. R., and Muskavitch, M. A. (1995). Relationships between complex Delta expression and the specification of retinal cell fates during *Drosophila* eye development. Mech. Dev. *50*, 201–216.

Peplowska, K., Markgraf, D. F., Ostrowicz, C. W., Bange, G., and Ungermann, C. (2007). The CORVET tethering complex interacts with the yeast Rab5 homolog Vps21 and is involved in endo-lysosomal biogenesis. Dev. Cell *12*, 739–750.

Peter, A.,- *et al*. (2002). Mapping and identification of essential gene functions on the X chromosome of Drosophila. EMBO Rep. *3*, 34–38.

Peterson, M. R., and Emr, S. D. (2001). The class C Vps complex functions at multiple stages of the vacuolar transport pathway. Traffic *2*, 476–486.

Pevsner, J., Hsu, S. C., Hyde, P. S., and Scheller, R. H. (1996). Mammalian homologues of yeast vacuolar protein sorting (*vps*) genes implicated in Golgi-to-lysosome trafficking. Gene *183*, 7–14.

Piper, R. C., Whitters, E. A., and Stevens, T. H. (1994). Yeast Vps45p is a Sec1p-like protein required for the consumption of vacuole-targeted, post-Golgi transport vesicles. Eur. J. Cell Biol. *65*, 305–318.

Poupon, V., Stewart, A., Gray, S. R., Piper, R. C., and Luzio, J. P. (2003). The role of mVps18p in clustering, fusion, and intracellular localization of late endocytic organelles. Mol. Biol. Cell *14*, 4015–4027.

Pulipparacharuvil, S., Akbar, M. A., Ray, S., Sevrioukov, E. A., Haberman, A. S., Rohrer, J., and Krämer, H. (2005). *Drosophila* Vps16A is required for trafficking to lysosomes and biogenesis of pigment granules. J. Cell Sci. *118*, 3663–3673.

Richardson, S. C., Winistorfer, S. C., Poupon, V., Luzio, J. P., and Piper, R. C. (2004). Mammalian late vacuole protein sorting orthologues participate in early endosomal fusion and interact with the cytoskeleton. Mol. Biol. Cell *15*, 1197–1210.

Rieder, S. E., and Emr, S. D. (1997). A novel RING finger protein complex essential for a late step in protein transport to the yeast vacuole. Mol. Biol. Cell *8*, 2307–2327.

Rink, J., Ghigo, E., Kalaidzidis, Y., and Zerial, M. (2005). Rab conversion as a mechanism of progression from early to late endosomes. Cell *122*, 735–749.

Rizo, J., and Sudhof, T. C. (2002). Snares and Munc18 in synaptic vesicle fusion. Nat. Rev. Neurosci. *3*, 641–653.

Rubinsztein, D. C. (2006). The roles of intracellular protein-degradation pathways in neurodegeneration. Nature *443*, 780–786.

Sato, T. K., Rehling, P., Peterson, M. R., and Emr, S. D. (2000). Class C Vps protein complex regulates vacuolar SNARE pairing and is required for vesicle docking/fusion. Mol. Cell *6*, 661–671.

Seals, D. F., Eitzen, G., Margolis, N., Wickner, W. T., and Price, A. (2000). A Ypt/Rab effector complex containing the Sec1 homolog Vps33p is required for homotypic vacuole fusion. Proc. Natl. Acad. Sci. USA *97*, 9402–9407.

Seto, E. S., Bellen, H. J., and Lloyd, T. E. (2002). When cell biology meets development: endocytic regulation of signaling pathways. Genes Dev. *16*, 1314–1336.

Sevrioukov, E. A., He, J. P., Moghrabi, N., Sunio, A., and Krämer, H. (1999). A role for the *deep orange* and *carnation* eye color genes in lysosomal delivery in *Drosophila*. Mol. Cell *4*, 479–486.

Sevrioukov, E. A., Moghrabi, N., Kuhn, M., and Krämer, H. (2005). A mutation in dVps28 reveals a link between a subunit of the endosomal sorting complex required for transport-I complex and the actin cytoskeleton in *Drosophila*. Mol. Biol. Cell *16*, 2301–2312.

Shacka, J. J., Klocke, B. J., Young, C., Shibata, M., Olney, J. W., Uchiyama, Y., Saftig, P., and Roth, K. A. (2007). Cathepsin D deficiency induces persistent neurodegeneration in the absence of Bax-dependent apoptosis. J. Neurosci. *27*, 2081–2090.

Shen, J., Tareste, D. C., Paumet, F., Rothman, J. E., and Melia, T. J. (2007). Selective activation of cognate SNAREpins by Sec1/Munc18 proteins. Cell *128*, 183–195.

Shestopal, S. A., Makunin, I. V., Belyaeva, E. S., Ashburner, M., and Zhimulev, I. F. (1997). Molecular characterization of the *deep orange* (*dor*) gene of *Drosophila melanogaster*. Mol. Gen. Genet. *253*, 642–648.

Silver, S. J., and Rebay, I. (2005). Signaling circuitries in development: insights from the retinal determination gene network. Development *132*, 3–13.

Simonsen, A., Cumming, R. C., Lindmo, K., Galaviz, V., Cheng, S., Rusten, T. E., and Finley, K. D. (2007). Genetic modifiers of the *Drosophila* blue cheese gene link defects in lysosomal transport with decreased life span and altered ubiquitinated-protein profiles. Genetics *176*, 1283–1297.

Simpson, F., Peden, A. A., Christopoulou, L., and Robinson, M. S. (1997). Characterization of the adaptor-related protein complex, AP-3. J. Cell Biol. *137*, 835–845.

Sriram, V., Krishnan, K. S., and Mayor, S. (2003). deep-orange and carnation define distinct stages in late endosomal biogenesis in *Drosophila melanogaster*. J. Cell Biol. *161*, 593–607.

Stroupe, C., Collins, K. M., Fratti, R. A., and Wickner, W. (2006). Purification of active HOPS complex reveals its affinities for phosphoinositides and the SNARE Vam7p. EMBO J. *25*, 1579–1589.

Subrahmanyam, G., Rudd, C. E., and Schneider, H. (2003). Association of T cell antigen CD7 with type II phosphatidylinositol-4 kinase, a key component in pathways of inositol phosphate turnover. Eur. J. Immunol. *33*, 46–52.

Subramanian, S., Woolford, C. A., and Jones, E. W. (2004). The Sec1/Munc18 protein, Vps33p, functions at the endosome and the vacuole of *Saccharomyces cerevisiae*. Mol. Biol. Cell *15*, 2593–2605.

Suzuki, T., Oiso, N., Gautam, R., Novak, E. K., Panthier, J. J., Suprabha, P. G., Vida, T., Swank, R. T., and Spritz, R. A. (2003). The mouse organellar biogenesis mutant buff results from a mutation in Vps33a, a homologue of yeast vps33 and *Drosophila* carnation. Proc. Natl. Acad. Sci. USA *100*, 1146–1150.

Thompson, B. J., Mathieu, J., Sung, H. H., Loeser, E., Rorth, P., and Cohen, S. M. (2005). Tumor suppressor properties of the ESCRT-II complex component Vps25 in *Drosophila*. Dev. Cell *9*, 711–720.

Toonen, R. F., and Verhage, M. (2003). Vesicle trafficking: pleasure and pain from SM genes. Trends Cell Biol. *13*, 177–186.

Vaccari, T., and Bilder, D. (2005). The *Drosophila* tumor suppressor vps25 prevents nonautonomous overproliferation by regulating notch trafficking. Dev. Cell *9*, 687–698.

Van Vactor, D.L.J., Cagan, R. L., Krämer, H., and Zipursky, S. L. (1991). Induction in the developing compound eye of *Drosophila*: multiple mechanisms restrict R7 induction to a single retinal precursor cell. Cell *67*, 1145–1155.

Wang, L., Merz, A. J., Collins, K. M., and Wickner, W. (2003). Hierarchy of protein assembly at the vertex ring domain for yeast vacuole docking and fusion. J. Cell Biol. *160*, 365–374.

Wang, T., and Montell, C. (2007). Phototransduction and retinal degeneration in Drosophila. Pflugers Arch.

Warner, T. S., Sinclair, D. A., Fitzpatrick, K. A., Singh, M., Devlin, R. H., and Honda, B. M. (1998). The light gene of *Drosophila melanogaster* encodes a homologue of VPS41, a yeast gene involved in cellular-protein trafficking. Genome *41*, 236–243.

Whyte, J. R., and Munro, S. (2002). Vesicle tethering complexes in membrane traffic. J. Cell Sci. *115*, 2627–2637.

Wodarz, A., Hinz, U., Engelbert, M., and Knust, E. (1995). Expression of crumbs confers apical character on plasma membrane domains of ectodermal epithelia of *Drosophila*. Cell *82*, 67–76.

Wucherpfennig, T., Wilsch-Brauninger, M., and Gonzalez-Gaitan, M. (2003). Role of *Drosophila* Rab5 during endosomal trafficking at the synapse and evoked neurotransmitter release. J. Cell Biol. *161*, 609–624.

Wurmser, A. E., Sato, T. K., and Emr, S. D. (2000). New component of the vacuolar class C-Vps complex couples nucleotide exchange on the Ypt7 GTPase to SNARE-dependent docking and fusion. J. Cell Biol. *151*, 551–562.

Xu, H., Boulianne, G. L., and Trimble, W. S. (2002). Drosophila syntaxin 16 is a Q-SNARE implicated in Golgi dynamics. J. Cell Sci. *115*, 4447–4455.

Xu, T., and Rubin, G. M. (1993). Analysis of genetic mosaics in developing and adult *Drosophila* tissues. Development *117*, 1223–1237.